



## CHARACTERIZATION OF FINE CARBONACEOUS AEROSOLS FROM THE EASTERN MEDITERRANEAN: CONTRIBUTIONS OF FOSSIL AND NON-FOSSIL CARBON SOURCES

Chandra Mouli Pavuluri<sup>1,2\*</sup>  • Nikolaos Mihalopoulos<sup>1,3,4</sup> • Masao Uchida<sup>5</sup>  • Kanako Mantoku<sup>5</sup> • Toshiyuki Kobayashi<sup>5</sup> • Pingqing Fu<sup>1,2</sup> • Kimitaka Kawamura<sup>1,6\*</sup>

<sup>1</sup>Institute of Low Temperature Science, Hokkaido University, Sapporo 060-0819, Japan

<sup>2</sup>Institute of Surface-Earth System Science, School of Earth System Science, Tianjin University, Tianjin 300072, China

<sup>3</sup>Environmental Chemical Processes Laboratory, University of Crete, GR-71003, Crete, Greece

<sup>4</sup>National Observatory of Athens, Athens, Greece

<sup>5</sup>AMS Facility (NIES-TERRA), Earth System Division, National Institute for Environmental Studies, Tsukuba, Japan

<sup>6</sup>Now at Chubu Institute for Advanced Studies, Chubu University, Kasugai 487-8501, Japan

**ABSTRACT.** In order to better characterise carbonaceous components in atmospheric aerosols and to assess the contributions of fossil carbon (FC) and non-fossil carbon (NFC) sources and their seasonality in the Eastern Mediterranean, we collected fine (PM<sub>1.3</sub>) aerosols at a remote marine background site, the Finokalia Research Station, Crete, Greece, over a period of one-year. PM<sub>1.3</sub> samples were analysed for elemental carbon (EC), organic carbon (OC), water-soluble OC (WSOC), and stable carbon isotope ratio ( $\delta^{13}\text{C}_{\text{TC}}$ ) and radiocarbon content ( $^{14}\text{C}_{\text{TC}}$ ) (pMC) of total carbon (TC). All the parameters, i.e., PM<sub>1.3</sub>,  $\delta^{13}\text{C}_{\text{TC}}$  and  $^{14}\text{C}_{\text{TC}}$  showed a clear temporal pattern with higher values in summer and lower values in autumn. The  $^{14}\text{C}_{\text{TC}}$  ranged from 54.7 to 99.1 pMC with an average of 74.5 pMC during the entire year. The FC content in TC (FC<sub>TC</sub>) was found to be slightly lower in winter and almost stable in other seasons, whereas the NFC contents (NFC<sub>TC</sub>) showed a clear seasonality with the highest level in summer followed by spring and the lowest level in winter. Based on these results together with the seasonal distributions of organic tracers, we found that biomass burning (BB) and soil dust are two major sources of the fine aerosols in winter. Although biogenic emissions of VOCs followed by subsequent secondary oxidation processes are significant in summer followed by spring and autumn, pollen is a significant contributor to TC in spring. This study showed that emissions from fossil fuel combustion are significant (25.5%) but minor compared to NFC sources in the eastern Mediterranean.

**KEYWORDS:**  $^{13}\text{C}$  and  $^{14}\text{C}$  isotope ratios, carbonaceous components, Eastern Mediterranean, PM<sub>1.3</sub>.

## INTRODUCTION

Carbonaceous aerosols: elemental carbon (EC) and organic carbon (OC), scatter and absorb the solar radiation and act as cloud condensation nuclei (CCN), seriously affecting the Earth's climate system (Carmichael et al. 2009; Menon et al. 2002; Novakov and Penner 1993; Ramanathan et al. 2001; Rosenfeld et al. 2019). They also have adverse effects on human health with increased morbidity and mortality (Nel 2005; Lin et al. 2017; Arfin et al. 2023) and play an important role in atmospheric chemistry (Kolb and Worsnop 2012). EC directly emits from sources such as fossil fuel combustion, biomass burning (BB) and soil dust (primary). While organic aerosols (OA, generally measured as OC) are emitted directly from primary sources and are also formed by photo-oxidation of volatile organic compounds (VOCs) emitted from both anthropogenic and biogenic sources, these are so called secondary OA (SOA) (Baltensperger et al. 2005; Robinson et al. 2007; Srivastava et al. 2022). The OA are estimated to account for a large fraction (20–90%) of the submicron aerosols (Kanakidou et al. 2005). In addition, both BB emissions and secondary formation and transformation of OA contribute to the high loading of water-soluble OC (WSOC), which further enhances the indirect climate effect of OA. However, the contribution of anthropogenic sources to OA are estimated to be

\*Corresponding authors. Emails: [cmpavuluri@tju.edu.cn](mailto:cmpavuluri@tju.edu.cn) & [kkawamura@isc.chubu.ac.jp](mailto:kkawamura@isc.chubu.ac.jp)

~50% at northern mid-latitudes and even higher in densely populated areas such as North America, Western Europe, and East Asia (de Gouw and Jimenez 2009).

It is well established that the stable carbon isotope ratios of total carbon ( $\delta^{13}\text{C}_{\text{TC}}$ ) highly depend on its sources, with an obvious difference in the isotopic signatures of the particles derived from different sources. Indeed the particles of marine origin are highly enriched with  $^{13}\text{C}$  (Chesselet et al. 1981; Cachier et al. 1985; Miyazaki et al. 2011), with  $\delta^{13}\text{C}$  that are different from those of the particles of continental origin, especially anthropogenic sources (Turekian 2003; Cao et al. 2011). Therefore,  $\delta^{13}\text{C}_{\text{TC}}$  of aerosols is useful for investigating their origin and has been used in several studies in the last two decades (Rudolph 2002; Pavuluri et al. 2011b; Dong et al. 2023).

Although radiocarbon ( $^{14}\text{C}$ ) is well known for providing chronologies through dating method, its application has been extended much further to investigate the fundamental relationships between different compartments of the Earth and climate system (Heaton et al. 2021). Because  $^{14}\text{C}$  decays with a half-life of 5730 years, the  $^{14}\text{C}$  is completely absent in carbonaceous aerosols derived from fossil fuel sources, whereas that derived from modern materials (e.g., biomass burning and biological emissions) contain the  $^{14}\text{C}$  at contemporary or near contemporary level. Therefore, measurement of the  $^{14}\text{C}/^{12}\text{C}$  ratio in aerosols has become a unique tool to unambiguously apportion the fossil (FC) and non-fossil carbon (NFC) contents in the atmospheric aerosols (Szidat et al. 2004; Gustafsson et al. 2009; Pavuluri et al. 2013; Kirillova et al. 2014; Liu et al. 2016; Song et al. 2019; Li et al. 2022; Lim et al. 2022). However, the  $^{14}\text{C}$  data alone cannot distinguish different sources of the NFC.

A combined study of  $^{14}\text{C}$  with elemental and molecular tracers has been shown to be an excellent technique to identify and apportion the different sources of NFC: biomass burning, biological emissions, and SOA from biogenic VOCs (Gelencsér et al. 2007; Pavuluri et al. 2013). However, the sources of carbonaceous aerosols are still poorly understood due to a lack of long-term  $^{14}\text{C}$  measurements and/or limited studies on organic molecular tracers (Gilardoni et al. 2011; Yttri et al. 2019), which provide more specific source information: fatty acids are emitted from terrestrial plant wax, vascular plants, microbes, and marine phytoplankton. Levoglucosan is formed during the pyrolysis of cellulose. Biological materials such as pollen, fungi, and bacteria consist of sucrose and mannitol. Isoprene,  $\alpha$ -pinene and  $\beta$ -caryophyllene produce SOA upon oxidation in the atmosphere (Simoneit et al. 2004; Fu et al. 2010; Wang et al. 2019).

The eastern Mediterranean is considered as an important region for atmospheric aerosol studies, where the aerosol radiative forcing is among the highest in the world, especially in summer (Lelieveld et al. 2002; Urdiales-Flores et al. 2023). It has also been reported that the radiative cooling effect of aerosols is up to 5 times greater than the warming caused by greenhouse gases (Vrekoussis et al. 2005), and the radiative forcing is also varies significantly from season-to-season due to weather conditions and the origin of air masses (Stock et al. 2011). Much attention has been paid to the aerosols of eastern Mediterranean with both short and long term measurements. It has been found that the organic fraction accounts for one third of the submicron aerosols in summer, and its contribution from biomass burning is dominant during March-April and July-September, based on the elemental tracers and mass fractions of carbonaceous components, together with the origins of air masses (Lelieveld et al. 2002; Sciare et al. 2008; Paraskevopoulou et al. 2014). However, the contributions of FC and NFC to total carbon (TC), the nature of the different FC and NFC sources (biomass burning and biogenic)

and the atmospheric processing of aerosols in the eastern Mediterranean troposphere and the entire southern Europe are not yet fully understood.

The aim of this study is to present the characteristics of carbonaceous components,  $^{13}\text{C}$  and  $^{14}\text{C}$  isotope ratios of TC in fine aerosols ( $\text{PM}_{1.3}$ ) over a one-year period and to apportion the fossil and non-fossil contents of TC in  $\text{PM}_{1.3}$  in the eastern Mediterranean troposphere. The results are discussed together with the observations of organic molecular marker species in order to assess the importance of various FC and NFC sources and the atmospheric processing (aging) of carbonaceous aerosols over the Mediterranean region.

## EXPERIMENTAL

### Aerosol Sampling

$\text{PM}_{1.3}$  sampling was carried out at a remote marine background site, the Finokalia Research Station, characterizing the eastern Mediterranean troposphere and located at  $35^{\circ}32'\text{N}$ ,  $25^{\circ}67'\text{E}$  (<http://finokalia.chemistry.uoc.gr>) on a hill (250 m above sea level) facing the sea on the northern coast of the Island of Crete, Greece (Kouvarakis et al. 2002). Aerosol samples were collected using a virtual impactor (VI) (Loo and Cork 1988), modified to divide particles into two size fractions: fine (aerodynamic particle diameter  $D_a < 1.3 \mu\text{m}$ ) and coarse particles ( $D_a > 1.3 \mu\text{m}$ ). The inlet preceding each VI has a cut-off size of  $10 \mu\text{m}$ . The operational flow rate is  $16.7 \text{ L min}^{-1}$  divided into 1.7 and 15.0 minor and major flows, respectively. More details can be found from Koulouri et al. (2008).  $\text{PM}_{1.3}$  samples were collected on a weekly basis for two consecutive days each from October 2009 to October 2010 ( $n = 51$ ) using pre-combusted ( $450^{\circ}\text{C}$  for 6 hr) quartz fiber filters (Whatman Q-MA; 47 mm in diameter). Filter samples were wrapped in aluminium foil, sealed in plastic boxes and stored in dark at  $-20^{\circ}\text{C}$  until chemical analysis.

The aerosol mass in each filter was measured gravimetrically using analytical balance (Mettler-Toledo; AB204) by the difference in mass of the filters before and after sampling, which had been conditioned in a desiccator for approximately 48 hr.

### Measurements of Carbonaceous Components and $\delta^{13}\text{C}_{\text{TC}}$

EC and OC were measured using an EC/OC analyzer (Sunset Laboratory Inc., USA) following the Interagency Monitoring Protected Visual Environments (IMPROVE) thermal/optical evolution protocol and a non-dispersive infrared (NDIR) detector system as described elsewhere (Pavuluri et al. 2011a). Briefly, the transmittance of laser light (660 nm) through the filter punch (1 cm in diameter) was used to establish the OC/EC split point and hence the OC correction. In addition, the carbonate carbon (CC) was estimated by manual integration of the last (OC4) peak appearing at the maximum temperature step and was subtracted from the total OC (Kaskaoutis et al. 2020) to avoid any bias in the OC. The analytical errors in duplicate analyses were within 0.7% for OC and 4.3% for EC.

To measure the WSOC, an aliquot of the filter disc (1 cm in diameter) was extracted with 10 ml organic free Milli Q water ( $18.3 \text{ M}\Omega$ ) under ultrasonication for 20 min. The extracts were then passed through syringe filter (Millex-GV, 0.45  $\mu\text{m}$ , Millipore) and then WSOC was measured using TOC analyzer (Shimadzu TOC- $\text{VCSH}$ ). The analytical error in duplicate analyses was within 9%.

$\delta^{13}\text{C}_{\text{TC}}$  was determined using an elemental analyzer (EA, Carlo Erba NA 1500) coupled to stable isotope ratio mass spectrometer (irMS, Finnigan MAT Delta Plus) as described

elsewhere (Pavuluri et al. 2011b). Briefly, an aliquot of filter packed in a tin cup was injected into EA and the derived gases: CO<sub>2</sub> (and N<sub>2</sub>), were transferred to irMS via ConFlo-II to measure the <sup>13</sup>C/<sup>12</sup>C in TC. The δ<sup>13</sup>C<sub>TC</sub> values relative to Pee Dee Belemnite (PDB) were calculated using the following formula:

$$\delta^{13}\text{C}_{\text{TC}} = \left[ \left( \frac{^{13}\text{C}/^{12}\text{C}}{\text{sample}} \right) / \left( \frac{^{13}\text{C}/^{12}\text{C}}{\text{standard}} \right) - 1 \right] \times 1000.$$

The water-insoluble OC (WIOC) was estimated from the difference between OC and WSOC. The sum of EC, OC and CC was considered as TC.

The secondary OC (SOC) was estimated based on the EC tracer method (Castro et al. 1999; Pavuluri et al. 2011a), although it involves some degree of uncertainty, using the minimum value of OC/EC ratio obtained during the campaign as follows:

$$[\text{SOC}] = [\text{OC}]_{\text{meas}} - ([\text{EC}]_{\text{meas}} \times (\text{OC/EC})_{\text{min}})$$

The minimum OC/EC ratios of 2.11 for the whole campaign period and 2.65, 2.84, 2.38 and 2.11 for the autumn, winter, spring and summer periods respectively were used as (OC/EC)<sub>min</sub> and the primary OC (POC) contribution from non-combustion sources was assumed to be negligible. Therefore, the SOC results obtained, and the conclusions drawn from them would not be significantly affected.

### Determination of Radiocarbon in TC

The radiocarbon content in the TC (<sup>14</sup>C<sub>TC</sub>) of PM<sub>1.3</sub> was determined using an accelerator mass spectrometer (AMS), as described elsewhere (Pavuluri et al. 2013). Briefly, the carbon of a filter disc (1.0 cm in diameter) was combusted at 850°C for 5 hr in a quartz tube (25 cm × 9 mm o.d.) with copper oxide and elemental silver wires, and the CO<sub>2</sub> produced was reduced to make a graphite target for AMS analysis in an automated microscale graphitization vacuum line (Uchida et al. 2010). <sup>14</sup>C contents were measured using the 5MV Pelletron accelerator mass spectrometer (15SDH-2, National Electrostatic Cooperation, Middleton, USA) at the NIES-TERRA AMS facility, the National Institute for Environmental Studies (NIES) (Uchida et al. 2004, 2023). All <sup>14</sup>C<sub>TC</sub> are expressed as percentage of modern (non-fossil) carbon (pMC) (Stuiver and Polach 1977), with δ<sup>13</sup>C correction. The pMC values were calculated by normalisation to the standard material NIST SRM 4990c (HOX II) with a known pMC value (=134.07) as:

$$\text{pMC} = \left[ \left( \frac{^{14}\text{C}/^{12}\text{C}}{\text{sample}} \right) / \left( 0.749 \times \left( \frac{^{14}\text{C}/^{12}\text{C}}{\text{HOX II}} \right) \right) \right] \times 100$$

The carbon amount was quantified manometrically from CO<sub>2</sub> gas after combustion. We have not corrected the <sup>14</sup>C results for the blank filter. The amount of TC derived from an untreated blank filter was less than 0.42 ± 0.21 μgC (*n* = 3), which represents at most less than 1% of the TC (50–300 μgC) in each sample, and therefore the blank contribution was considered to be negligible.

### Measurements of Organic Molecular Markers

Organic molecular marker species were measured as described elsewhere (Fu et al. 2010). Briefly, the organic species were extracted three times with dichloromethane/methanol (2:1; v/v) under ultrasonication for 10 min each and the extracts were concentrated to dryness and then derivatized with 50 mL of N,O-bis-(trimethylsilyl)-trifluoroacetamide (BSTFA) containing 1% trimethylsilyl chloride and 10 mL of pyridine at 70°C for 3 hr.

The derivatives were diluted to 140 mL with *n*-hexane containing 1.43 ng mL<sup>-1</sup> of the internal standard (C<sub>13</sub> *n*-alkane) and then analyzed using a capillary gas chromatograph (Hewlett-Packard 6890) coupled to a mass spectrometer (Hewlett-Packard 5973) (GC/MS). The recoveries for the authentic standards and surrogates were better than 80% and the analytical errors in duplicate analyses were less than 10%.

## RESULTS AND DISCUSSION

### PM<sub>1.3</sub> and Carbonaceous Components and Their Temporal Variations

The atmospheric load of PM<sub>1.3</sub> and the concentrations of carbonaceous components in the PM<sub>1.3</sub> during the whole campaign period (annual) and in each season: autumn (September–November), winter (December–February), spring (March–May) and summer (June–August), are summarized in Table 1. Their temporal variations are depicted in Figure 1. The PM<sub>1.3</sub> concentrations varied between 3.36 and 23.9 µgm<sup>-3</sup> during the campaign (Table 1) and showed a clear temporal trend with lower values in autumn followed by a gradual increase to maximum in summer and then a sharp decrease in autumn, peaking abruptly in late autumn 2009 and during late winter and early spring 2010 (Figure 1d). On average, the PM<sub>1.3</sub> was highest in summer followed by spring and lowest in winter (Table 1).

Temporal variations of TC and all the organic components: OC, WSOC, SOC and WIOC, were very similar to each other and similar to those of PM<sub>1.3</sub>, except for its abrupt peaks during late winter and early spring (Figure 1b–d). The temporal trend of EC was also generally similar to that of TC and OC, except during the months February, March and September 2010, when EC was almost negligible (Figure 1a, c). On average, all the carbonaceous components: WSOC, OC and TC, as well as EC, were much higher in summer followed by spring and lower in winter, again similar to the seasonality of PM<sub>1.3</sub> (Table 1). On the other hand, TC accounted for 9.10 ± 2.91% (range, 3.41 to 16.2%) in PM<sub>1.3</sub> during the campaign, with an almost equal contribution in each season: 8.36 ± 2.23%, 8.50 ± 3.68%, 9.00 ± 2.36% and 10.6 ± 3.45% in autumn, winter, spring and summer, respectively. Such similarities in the temporal patterns and seasonality among the carbonaceous components as well as with those of PM<sub>1.3</sub> from Crete, suggest that the PM<sub>1.3</sub> loading and its composition in the eastern Mediterranean atmosphere were derived from the emissions of the distant source and intensively aged during the long-range atmospheric transport, and hence this study provides the regional scenario.

Interestingly, the temporal pattern of the manually estimated CC was found to be exactly the same as that of the OC (Figure 1a, c). Such similarity suggests that most of the estimated CC in Crete aerosols might be OC, but not the CC. Therefore, it is likely that the OC reported here may be underestimated. In fact, the abundance of WSOC in OC (range: 48.5–131%; ave. 77.5 ± 13.2%) was exceeded the 100% in 2 autumn samples, confirming that the OC was underestimated in this study. However, in order to avoid any possible bias in OC quantification, we considered keeping only the C content estimated from the final step of the inert-mode temperature protocol (OC4 fraction) as CC (Kaskaoutis et al. 2020) only. The fraction of SOC in OC was up to 97.6% with an average of 64.1 ± 25.7% during the campaign with a higher contribution in winter (70.9 ± 30.5%), followed by autumn (63.2 ± 28.0%), summer (59.6 ± 23.7) and lower in spring (43.5 ± 31.4%). The higher SOC/OC in winter rather than in summer suggests that the secondary processes are more intensive in winter as well and/or that the contribution of EC from major sources such as BB may be much lower in winter and autumn in the eastern Mediterranean.

Table 1 Annual and seasonal summary of the concentrations of carbonaceous components and PM<sub>1,3</sub> (µgm<sup>-3</sup>), δ<sup>13</sup>C<sub>TC</sub> (‰) and <sup>14</sup>C<sub>TC</sub> (pMC) in the PM<sub>1,3</sub> from Finokalia, Crete Island, Greece, the Eastern Mediterranean during October 2009–October 2010. See text for abbreviations.

	Annual		Autumn		Winter		Spring		Summer	
	Range	Ave. ± SD	Range	Ave. ± SD	Range	Ave. ± SD	Range	Ave. ± SD	Range	Ave. ± SD
Concentrations (µgm <sup>-3</sup> )										
EC	0.01–0.57	0.13 ± 0.12	0.02–0.17	0.07 ± 0.04	0.01–0.16	0.04 ± 0.05	0.02–0.43	0.18 ± 0.13	0.03–0.57	0.22 ± 0.15
OC	0.21–3.07	0.85 ± 0.60	0.21–1.51	0.66 ± 0.40	0.32–1.14	0.52 ± 0.27	0.32–1.36	0.83 ± 0.33	0.48–3.07	1.40 ± 0.87
CC	0.04–0.23	0.09 ± 0.04	0.04–0.14	0.08 ± 0.03	0.04–0.16	0.07 ± 0.04	0.05–0.23	0.10 ± 0.04	0.06–0.22	0.12 ± 0.05
WSOC	0.18–2.63	0.65 ± 0.47	0.21–1.02	0.50 ± 0.26	0.18–0.69	0.33 ± 0.16	0.30–0.96	0.63 ± 0.21	0.41–2.63	1.11 ± 0.68
WIOC	0.00–0.68	0.21 ± 0.17	0.00–0.55	0.16 ± 0.16	0.05–0.45	0.18 ± 0.13	0.03–0.61	0.20 ± 0.17	0.06–0.68	0.29 ± 0.21
SOC	0.00–2.33	0.58 ± 0.51	0.00–1.29	0.49 ± 0.39	0.00–1.09	0.39 ± 0.33	0.00–1.30	0.39 ± 0.40	0.00–2.33	0.93 ± 0.73
TC	0.30–3.87	1.07 ± 0.71	0.30–1.82	0.80 ± 0.44	0.38–1.24	0.63 ± 0.28	0.46–1.86	1.12 ± 0.41	0.79–3.87	1.75 ± 1.01
PM <sub>1,3</sub>	3.36–23.9	11.8 ± 5.18	4.37–18.8	10.1 ± 4.70	3.36–23.19	8.55 ± 6.22	7.75–23.3	12.4 ± 4.03	10.3–23.9	15.4 ± 4.24
Isotope ratios										
δ <sup>13</sup> C <sub>TC</sub> (‰)	–26.5–(–)21.1	–24.4 ± 1.00	–26.5–(–)23.0	–24.6 ± 0.97	–26.1–(–)22.2	–24.9 ± 1.30	–24.9–(–)21.1	–24.0 ± 0.96	–25.8–(–)23.4	–24.4 ± 0.70
<sup>14</sup> C <sub>TC</sub> (pMC)	54.7–99.1	74.5 ± 10.6	54.7–75.8	66.7 ± 8.89	69.9–81.3	75.6 ± 8.02	61.0–76.0	69.3 ± 6.34	69.0–99.1	82.8 ± 10.1



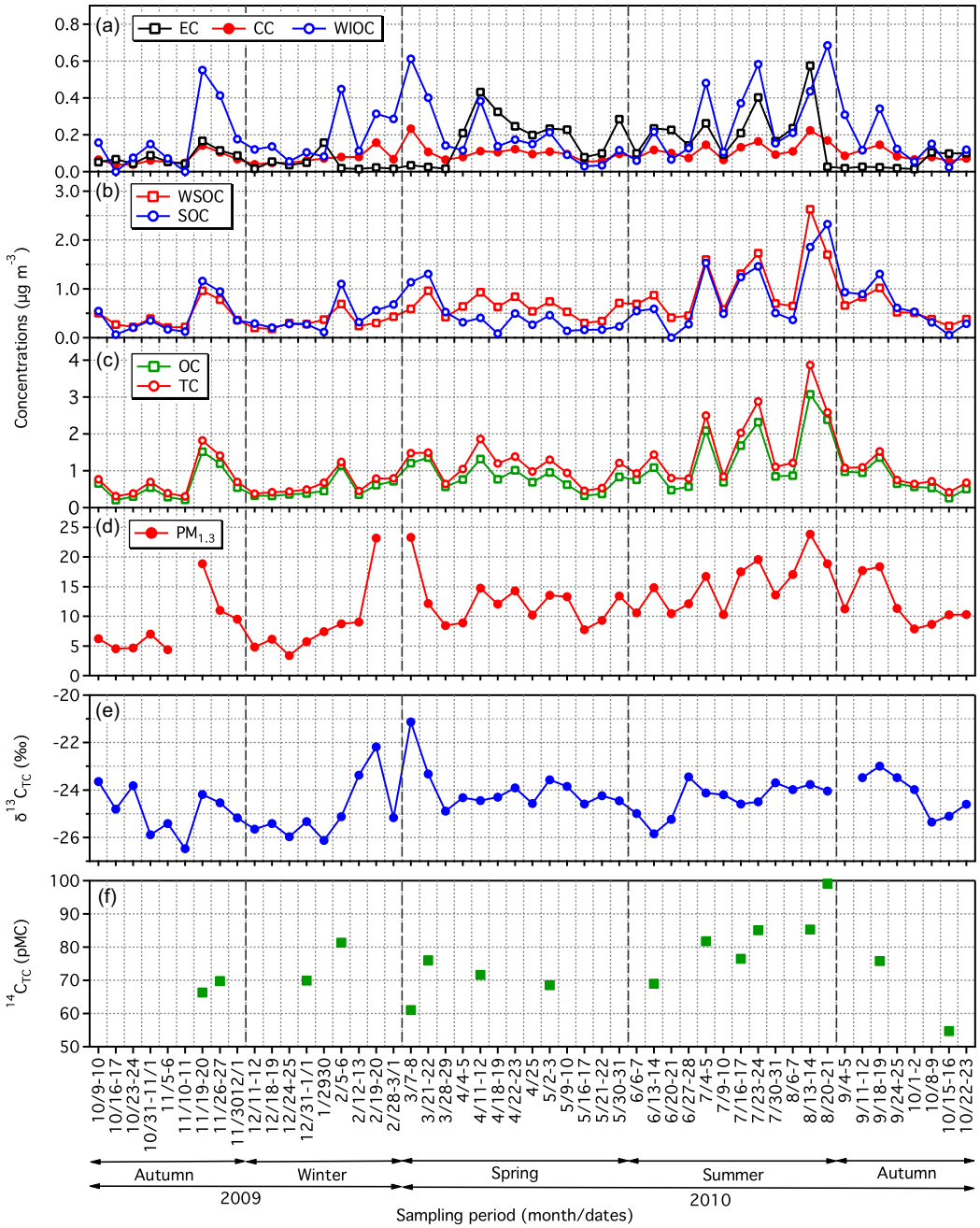


Figure 1 Temporal variations in concentrations of (a) EC, CC and WIOC, (b) WSOC and SOC, (c) OC and TC in PM<sub>1.3</sub> and (d) PM<sub>1.3</sub> mass, (e)  $\delta^{13}\text{C}_{\text{TC}}$  and (f)  $^{14}\text{C}_{\text{TC}}$  (pMC) in the PM<sub>1.3</sub> from Finokalia, Crete Island, Greece, the Eastern Mediterranean during October 2009–October 2010. See text for abbreviations.

### $\delta^{13}\text{C}_{\text{TC}}$ : Contributions of Continental and Marine Sources

The  $\delta^{13}\text{C}_{\text{TC}}$  values in  $\text{PM}_{1.3}$  ranged from  $-26.5$  to  $-21.1\text{‰}$  during the campaign and their temporal pattern did not show any seasonality, except for significantly higher values in few samples during late winter and early spring (Figure 1e), and their mean values were almost the same in all seasons (Table 1). The  $\delta^{13}\text{C}_{\text{TC}}$  in Crete are comparable to the isotopic signatures of the particles emitted by  $\text{C}_3$  plants biomass burning (BB) (range,  $-27.4$  to  $-23.8\text{‰}$ ) and fossil fuel combustion ( $-26.5 \pm 0.5\text{‰}$  to  $-24.2 \pm 0.6$ ), but not to those of  $\text{C}_4$  plants BB (range,  $-19.9$  to  $-13.8\text{‰}$ ) (Turekian et al. 1998; Widory et al. 2004). This comparability indicates that the eastern Mediterranean aerosols were mainly derived from the BB and fossil fuel combustion. Furthermore, the stability in the  $\delta^{13}\text{C}_{\text{TC}}$  independent to season and TC loadings during the campaign implies that the  $\text{PM}_{1.3}$  should have been derived from the same sources and subjected for intensive aging throughout the year.

However, since most of the area in this region is covered by the sea, it is important to estimate the possible contribution of marine sources to the carbonaceous aerosols in this region. It has been reported that  $\delta^{13}\text{C}_{\text{TC}}$  of  $-26.0\text{‰}$  and  $-21.0\text{‰}$  in atmospheric aerosols indicate the marine and continental origin, respectively (Cachier et al. 1985; Turekian 2003). As detailed in the previous section, the Crete aerosols were aged and therefore the  $^{13}\text{C}$  must be relatively enriched in the TC of  $\text{PM}_{1.3}$ . Therefore, we used the  $\delta^{13}\text{C}_{\text{TC}}$  of  $-26.5\text{‰}$  and  $-21.0\text{‰}$  as end-members of the continental and marine aerosols to calculate their relative contributions using the following equation:

$$\begin{aligned} \delta^{13}\text{C}_{\text{aerosol}} &= f_{\text{continental}} \times \delta^{13}\text{C}_{\text{continental}} + f_{\text{marine}} \times \delta^{13}\text{C}_{\text{marine}} \\ f_{\text{continental}} + f_{\text{marine}} &= 1 \end{aligned}$$

where  $f_{\text{continental}}$  and  $f_{\text{marine}}$  are the fractions of continental and marine carbon, respectively, and  $\delta^{13}\text{C}_{\text{continental}}$  and  $\delta^{13}\text{C}_{\text{marine}}$  are the  $\delta^{13}\text{C}$  values for end members.

The estimated contributions of continental carbon to TC in  $\text{PM}_{1.3}$  in the eastern Mediterranean ranged from 2.3–99.5% (ave.  $62.3 \pm 18.2\%$ ) during the campaign, with higher contributions in winter ( $71.4 \pm 23.6\%$ ), followed by autumn ( $64.7 \pm 17.7\%$ ) and summer ( $61.3 \pm 12.7\%$ ), and lower contributions in spring ( $54 \pm 17.4\%$ ). The average contribution of marine carbon to TC ( $37.7 \pm 18.2\%$ ) was close to that reported for marine aerosols at Bermuda (38%) (Turekian 2003) and close to that (45%) at the High Arctic (Narukawa et al. 2008), which was influenced by continental and marine sources. Thus, it is clear that the Crete aerosols originated mainly from continental sources such as fossil fuel combustion and BB and could also be of terrestrial biogenic emissions.

### Fossil and Non-Fossil Carbon Contents in TC: Implications for Sources

The  $^{14}\text{C}_{\text{TC}}$  ranged from 54.7 to 99.1 pMC during the campaign (Table 1) and showed a clear temporal pattern with a gradual increase from autumn to winter, followed by a decrease until late spring and then a gradual increase to a maximum in summer (Figure 1f). This temporal pattern was exactly similar to that of TC and other carbonaceous components and also  $\text{PM}_{1.3}$ , except for a few cases (Figure 1). Furthermore, TC concentrations showed a linear relationship with the  $^{14}\text{C}_{\text{TC}}$  (Figure 2a) and the correlation coefficient between them found to be relatively strong ( $r^2 = 0.50$ ;  $p = < 0.05$ ). Such similarities among the temporal trends of  $^{14}\text{C}_{\text{TC}}$ , carbonaceous components and  $\text{PM}_{1.3}$ , as well as the linear relationship between TC and  $^{14}\text{C}_{\text{TC}}$ , imply that the temporal changes in the atmospheric loadings of carbonaceous aerosols and



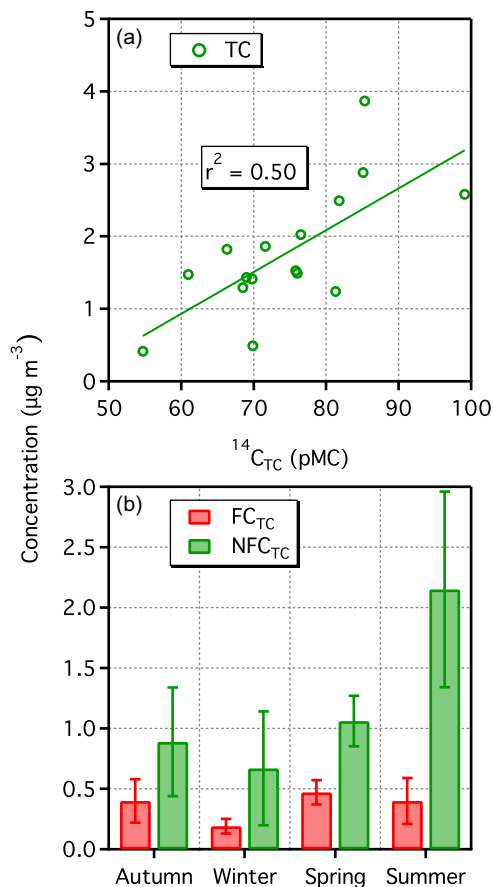


Figure 2 (a) Scatter plot between the concentrations of TC ( $\mu\text{g m}^{-3}$ ) and its  $^{14}\text{C}_{\text{TC}}$  (pMC) and seasonal changes in average concentrations (bars,  $\mu\text{g m}^{-3}$ , error bars show the standard deviation) of fossil ( $\text{FC}_{\text{TC}}$ ) and non-fossil carbon ( $\text{NFC}_{\text{TC}}$ ) contents in TC in  $\text{PM}_{1.3}$  from Finokalia, Crete Island, Greece, the eastern Mediterranean.

even the total  $\text{PM}_{1.3}$  in the eastern Mediterranean atmosphere were driven by the changes in their contributions from non-fossil carbon (NFC) sources such as BB and/or biogenic emissions and subsequent secondary processes. While their contributions from fossil carbon (FC) sources such as fossil fuel combustion emissions were almost stable throughout the year.

Seasonal averages of  $^{14}\text{C}_{\text{TC}}$  were found to be the highest in summer, followed by winter, spring and lower in autumn (Table 1). The second highest abundance of  $^{14}\text{C}_{\text{TC}}$  in winter is opposite to the seasonal averages of both carbonaceous components and  $\text{PM}_{1.3}$ , which showed the second highest abundance in spring and the lowest in winter (Table 1). The dissimilarity in the seasonal averages, particularly in winter, despite the similar temporal trends (Figure 1), between  $^{14}\text{C}_{\text{TC}}$  and the components of  $\text{PM}_{1.3}$  also suggests that the NFC sources such as BB must be important, but the amounts of carbonaceous particles and/or gaseous species emitted from these sources were not large in winter. To further investigate the role of NFC sources in the aerosol loading of the eastern Mediterranean atmosphere, we estimated the FC ( $\text{FC}_{\text{TC}}$ ) and NFC in TC ( $\text{NFC}_{\text{TC}}$ ) contents in the samples analyzed for  $^{14}\text{C}$  measurements ( $n = 16$ ) based on

the  $^{14}\text{C}_{\text{TC}}$ , and their averages are presented in Figure 2b. Interestingly, the averages of  $\text{FC}_{\text{TC}}$  were found to be almost equal in autumn, spring and summer and relatively lower in winter (Figure 2b). On the other hand, the average  $\text{NFC}_{\text{TC}}$  was found to be much higher in summer, followed by spring and autumn, and lower in winter (Figure 2b). However, the amount of  $\text{NFC}_{\text{TC}}$  was much higher than that of  $\text{FC}_{\text{TC}}$  in winter and the average mass ratios of the  $\text{NFC}_{\text{TC}}/\text{FC}_{\text{TC}}$  were  $2.16 \pm 0.80$  (median, 2.14),  $3.33 \pm 1.42$  (3.33),  $2.36 \pm 0.67$  (2.35) and  $21.8 \pm 42.8$  (5.10), in autumn, winter, spring and summer, respectively. In fact, the higher average mass ratio in summer was driven by an outlier (109).

These results clearly show that the contributions of NFC sources (including biogenic emissions) to atmospheric aerosols are very high compared to those of FC sources and vary significantly from season-to-season, thus controlling the seasonality of the atmospheric loadings of carbonaceous aerosols and also  $\text{PM}_{1,3}$  to a greater extent over the eastern Mediterranean. In fact, in contrast to our results, the previous studies reported that the anthropogenic sources such as fossil fuel combustion and BB emissions are the two main sources of aerosols in the eastern Mediterranean region (Lelieveld et al. 2002; Sciare et al. 2003, 2008), ignoring the role of biogenic emissions and subsequent secondary formation of the aerosols over this region.

We now examine the importance of NFC sources and subsequent secondary formation of carbonaceous aerosols, based on the seasonal changes in concentrations of molecular biomarkers (Figure 3, Pingqing Fu et al. unpublished data, personal communication). The lipid class compounds such as fatty acids are considered as biomarkers for understanding the importance of primary biological sources of atmospheric aerosols, and levoglucosan, formed during the pyrolysis of cellulose, is considered as a biomarker for BB (Simoneit et al. 2004; Fu et al. 2010). While the sum of species (see Figure 3 caption for list) derived from isoprene,  $\alpha$ -pinene,  $\beta$ -caryophyllene is considered as a biomarker for biogenic SOA, sucrose and mannitol are recognized as biomarkers for pollen and soil dust including microbes such as fungi and bacteria (Fu et al. 2010; Simoneit et al. 2004).

The molecular distributions of fatty acids showed a strong even carbon number predominance at  $\text{C}_{16}$  with Carbon Preference Index (CPI) ranging from 1.99–5.19 (ave. 3.21), suggesting that they are mostly derived from terrestrial higher plant waxes (Fu et al. 2010). The fatty acids load was abundant in all seasons with slightly higher levels in spring and summer (Figure 3), suggesting that the contributions of terrestrial biogenic emissions to OA are significant throughout the year with little increase during the growing season. Mean concentrations of levoglucosan were much higher in winter, followed by spring and autumn and lowest in summer, in agreement with Theodosi et al. 2018 (Figure 3). While the loadings of SOA derived from isoprene,  $\alpha$ -pinene and  $\beta$ -caryophyllene were much higher in summer followed by spring and autumn, and lowest in winter (Figure 3). Sucrose was abundant only in spring and lessor in other seasons, whereas mannitol was much higher in winter followed by spring and summer, and lowest in autumn (Figure 3).

In fact, the levels of NFC were always much higher than that of FC in each season during the campaign (Figure 2b). Despite the minute levels of biogenic SOA and lower levels of fatty acids in winter, the NFC was found to be relatively much higher than those of FC, compared in other seasons during the campaign (Figs. 2b and 3). Therefore, such higher levels of NFC in winter should have been driven mainly by biomass burning and soil dust, in addition to the primary biological emissions. In summer, the loadings of SOA derived from all the biogenic VOCs were much higher than in other seasons (Figure 3) and the NFC levels were almost doubled in

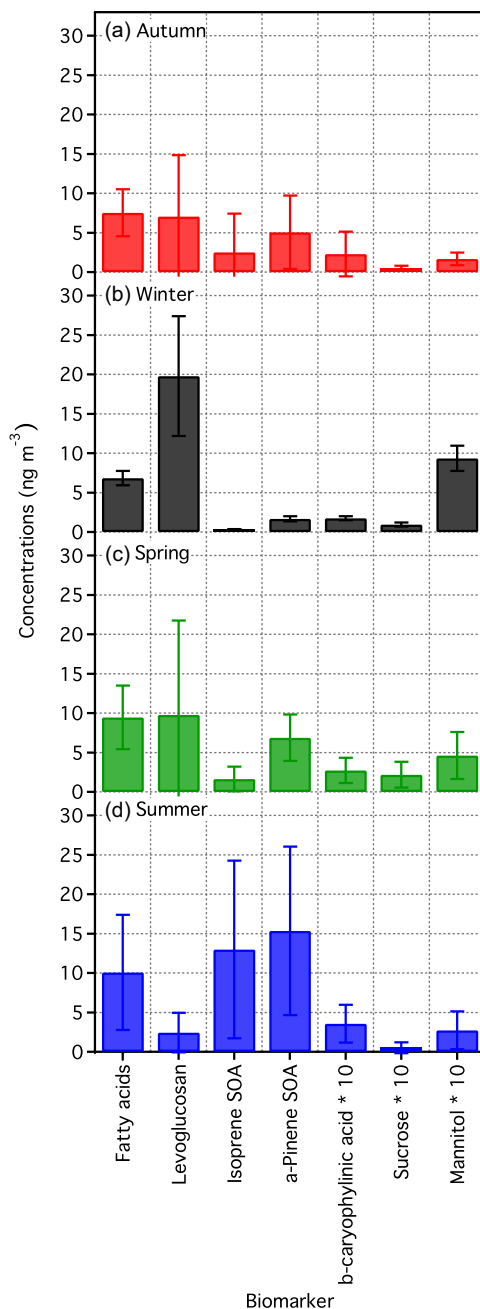


Figure 3 Total concentrations ( $\text{ng m}^{-3}$ ) of biomarker species: fatty acids ( $\Sigma\text{C}_8\text{-C}_{32}$ ), levoglucosan, isoprene- ( $\Sigma$ 2-methylglyceric acid+cis-2-methyl-1,3,4-trihydroxy-1-butene+3-methyl-2,3,4-trihydroxy-1-butene+trans-2-methyl-1,3,4-trihydroxy-1-butene+2-methylthreitol+2-methylerythritol) and  $\alpha$ -pinene-derived SOA ( $\Sigma$ 3-hydroxyglutaric acid+pinonic acid+pinic acid+3-methyl-1,2,3-butanetricarboxylic acid) species, and  $\beta$ -caryophyllinic acid, sucrose and mannitol in  $\text{PM}_{1,3}$  from Finokalia, Crete Island, Greece, the eastern Mediterranean in autumn (a), winter (b), spring (c) and summer (d).

summer to those in other seasons (Figure 2b), despite the minute levels of levoglucosan, sucrose and mannitol (Figure 3). Such a comparison between SOA and NFC clearly implies that the increment in the NFC loading must have mainly been driven by the SOA from biogenic VOCs, in addition to the primary biological emissions in summer.

The relatively high levels of NFC in spring and autumn, respectively (Figure 2b), are in consistence with the relatively high loadings of fatty acids, levoglucosan and  $\alpha$ -pinene SOA in those two seasons (Figure 3), implying that the emissions from biological sources including pollen, biomass burning and the SOA from terpenes should have been the major contributors in the spring and autumn periods. Such seasonal distributions of NFC and biomarkers together with the comparisons imply that the changes in the atmospheric loading of the NFC and thus the carbonaceous aerosols were mainly controlled by BB and biogenic emissions including soil dust and subsequent secondary formation processes in the eastern Mediterranean.

## CONCLUSIONS

This study presents the characteristics of carbonaceous components: EC, CC, WSOC, WIOC, SOC, OC and TC,  $\delta^{13}\text{C}_{\text{TC}}$  and  $^{14}\text{C}_{\text{TC}}$  in  $\text{PM}_{1.3}$  collected at a remote marine background site, the Finokalia Research Station on the Island of Crete, Greece in the eastern Mediterranean troposphere over a period of one year. Concentrations of carbonaceous components and  $\text{PM}_{1.3}$  as well as  $\delta^{13}\text{C}_{\text{TC}}$  and  $^{14}\text{C}_{\text{TC}}$  showed a clear seasonality during the campaign. The  $\delta^{13}\text{C}_{\text{TC}}$  revealed that the fraction of continental carbon is predominant in the eastern Mediterranean aerosols. The contributions of FC sources to carbonaceous aerosols are almost stable throughout the year, except in winter. On the other hand, the contributions of NFC sources to carbonaceous aerosols are much higher than those of the FC sources throughout the year, although they vary from season to season, thus controlling their seasonality. Furthermore, the contributions from BB and soil dust are higher in winter, while those from biogenic emissions and subsequent secondary processes are higher in summer, followed by spring and autumn. Pollen emissions are significant in spring. More importantly, these results show that although fossil fuel combustion emissions are significant, BB and biogenic emissions and their subsequent secondary processes are the main sources of carbonaceous aerosols in the eastern Mediterranean.

## ACKNOWLEDGMENTS

This study was in part supported by the Japan Society for the Promotion of Science (JSPS) through a Grant-in-Aid Nos. 21120510 and 24221001 and the Environment Research and Technology Development Fund (B-0903, B-0904) of the Ministry of the Environment, Japan, and National Natural Science Foundation of China (NSFC, Grant-in-Aid Nos.: 41775120 & 42277090), China. Measurements of carbonaceous components and organic molecular markers have been performed at Institute of Low Temperature Science, Hokkaido University, Sapporo 060-0819, and the  $^{14}\text{C}$  measurements were performed at the NIES-TERRA AMS Facility, National Institute for Environmental Studies, Tsukuba, Japan.

## COMPETING INTERESTS

The authors declare that they have no conflict of interest.

## REFERENCES

- Arfin T, Pillai AM, Mathew N, Tirpude A, Bang R, Mondal P. 2023. An overview of atmospheric aerosol and their effects on human health. *Environ Sci Pollut Res Int*.
- Baltensperger U, Kalberer M, Dommen J, Paulsen D, Alfarra MR, Coe H, Fisseha R, Gascho A, Gysel M, Nyeki S et al. 2005. Secondary organic aerosols from anthropogenic and biogenic precursors. *Faraday Discussions* 130.
- Cachier H, Buat-Menard P, Fontugne M, Rancher J. 1985. Source terms and source strengths of the carbonaceous aerosol in the tropics. *Journal of Atmospheric Chemistry* 3, 469–489. doi: [10.1007/BF00053872](https://doi.org/10.1007/BF00053872).
- Cao J-j, Chow JC, Tao J, Lee S-c, Watson JG, Ho K-f, Wang G-h, Zhu C-s, Han Y-m. 2011. Stable carbon isotopes in aerosols from chinese cities: influence of fossil fuels. *Atmospheric Environment* 45(6):1359–1363.
- Carmichael GR, Adhikary B, Kulkarni S, D’Allura A, Tang YH, Streets D, Zhang Q, Bond TC, Ramanathan V, Jamroensan A et al. 2009. Asian aerosols: Current and year 2030 distributions and implications to human health and regional climate change. *Environ Sci Technol*. 43(15):5811–5817.
- Castro L, Pio C, Harrison RM, Smith D. 1999. Carbonaceous aerosol in urban and rural european atmospheres: Estimation of secondary organic carbon concentrations. *Atmospheric Environment* 33(17):2771–2781.
- Chesselet R, Fontugne M, Buat-Ménard P, Ezat U, Lambert CE. 1981. The origin of particulate organic carbon in the atmosphere as indicated by its stable carbon isotopic composition. *Geophysical Research Letters* 8(4), 345–348. doi: [10.1029/GL008i004p00345](https://doi.org/10.1029/GL008i004p00345).
- de Gouw J, Jimenez JL. 2009. Organic aerosols in the Earth’s atmosphere. *Environ Sci Technol*. 43(20):7614–7618.
- Dong ZC, Pavuluri CM, Xu ZJ, Wang Y, Li PS, Fu PQ, Liu CQ. 2023. Measurement report: Chemical components and c and n isotoperatios of fine aerosols over tianjin, north china: Year-round observations. *Atmos Chem Phys*. 23(3):2119–2143.
- Fu PQ, Kawamura K, Pavuluri CM, Swaminathan T, Chen J. 2010. Molecular characterization of urban organic aerosol in Tropical India: Contributions of primary emissions and secondary photooxidation. *Atmospheric Chemistry and Physics* 10:2663–2689.
- Gelencsér A, May B, Simpson D, Sánchez-Ochoa A, Kasper-Giebl A, Puxbaum H, Caseiro A, Pio C, Legrand M. 2007. Source apportionment of pm2.5 organic aerosol over Europe: Primary/secondary, natural/anthropogenic, and fossil/biogenic origin. *Journal of Geophysical Research* 112(D23).
- Gilardoni S, Vignati E, Cavalli F, Putaud JP, Larsen BR, Karl M, Stenström K, Genberg J, Henne S, Dentener F. 2011. Better constraints on sources of carbonaceous aerosols using a combined <sup>14</sup>C – macro tracer analysis in a European rural background site. *Atmospheric Chemistry and Physics* 11(12):5685–5700.
- Gustafsson O, Kruså M, Zencak Z, Sheesley RJ, Granat L, Engström E, Praveen PS, Rao PSP, Leck C, Rodhe H. 2009. Brown clouds over South Asia: Biomass or fossil fuel combustion? *Science* 323:495–498.
- Heaton TJ, Bard E, Bronk Ramsey C, Butzin M, Kohler P, Muscheler R, Reimer PJ, Wacker L. 2021. Radiocarbon: A key tracer for studying Earth’s dynamo, climate system, carbon cycle, and sun. *Science* 374(6568):eabd7096.
- Kanakidou M, Seinfeld JH, Pandis SN, Barnes I, Dentener FJ, Facchini MC, Van Dingenen R, Ervens B, Nenes A, Nielsen CJ et al. 2005. Organic aerosol and global climate modelling: A review. *Atmospheric Chemistry and Physics* 5:1053–1123.
- Kaskaoutis DG, Grivas G, Theodosi C, Tsagkaraki M, Paraskevopoulou D, Stavroulas I, Liakakou E, Gkikas A, Hatzianastassiou N, Wu C. 2020. Carbonaceous aerosols in contrasting atmospheric environments in Greek cities: Evaluation of the ec-tracer methods for secondary organic carbon estimation. *Atmosphere* 11(2):161.
- Kirilova EN, Andersson A, Tiwari S, Srivastava AK, Bisht DS, Gustafsson Ö. 2014. Water-soluble organic carbon aerosols during a full new delhi winter: Isotope-based source apportionment and optical properties. *Journal of Geophysical Research: Atmospheres* 119(6):3476–3485.
- Kolb CE, Worsnop DR. 2012. Chemistry and composition of atmospheric aerosol particles. *Annu Rev Phys Chem*. 63:471–491.
- Koulouri E, Saarikoski S, Theodosi C, Markaki Z, Gerasopoulos E, Kouvarakis G, Mäkelä T, Hillamo R, Mihalopoulos N. 2008. Chemical composition and sources of fine and coarse aerosol particles in the Eastern Mediterranean. *Atmospheric Environment* 42(26):6542–6550.
- Kouvarakis G, Vrekoussis M, Mihalopoulos N, Kourtidis K, Rappengluck B, Gerasopoulos E, Zerefos C. 2002. Spatial and temporal variability of tropospheric ozone (O<sub>3</sub>) in the boundary layer above the Aegean Sea (Eastern Mediterranean). *Journal of Geophysical Research: Atmospheres* 107:8137.
- Lelieveld J, Berresheim H, Borrmann S, Crutzen PJ, Dentener FJ, Fischer H, Feichter J, Flatau PJ, Heland J, Holzinger R et al. 2002. Global air pollution crossroads over the mediterranean. *Science* 298(5594):794–799.
- Li C, Zhang C, Yan F, Kang S, Xu Y, Liu Y, Gao Y, Chen P, He C. 2022. Importance of local non-fossil sources to carbonaceous aerosols at the eastern fringe of the tibetan plateau, china:

- Delta(14)c and delta(13)c evidences. *Environ Pollut.* 311:119858.
- Lim S, Hwang J, Lee M, Czimczik CI, Xu X, Savarino J. 2022. Robust evidence of (14)C, (13)C, and (15)N analyses indicating fossil fuel sources for total carbon and ammonium in fine aerosols in seoul megacity. *Environ Sci Technol.* 56(11):6894–6904.
- Lin YH, Arashiro M, Clapp PW, Cui T, Sexton KG, Vizuete W, Gold A, Jaspers I, Fry RC, Surratt JD. 2017. Gene expression profiling in human lung cells exposed to isoprene-derived secondary organic aerosol. *Environ Sci Technol.* 51(14):8166–8175.
- Liu JW, Mo YZ, Li J, Liu D, Shen CD, Ding P, Jiang HY, Cheng ZN, Zhang XY, Tian CG et al. 2016. Radiocarbon-derived source apportionment of fine carbonaceous aerosols before, during, and after the 2014 Asia-Pacific Economic Cooperation (APEC) summit in Beijing, China. *J Geophys Res-Atmos.* 121(8):4177–4187.
- Loo BW, Cork CP. 1988. Development of high efficiency virtual impactors. *Aerosol Science and Technology* 9(3):167–176.
- Menon S, Hansen J, Nazarenko L, Luo Y. 2002. Climate effects of black carbon aerosols in china and india. *Science* 297(5590):2250–2253.
- Miyazaki Y, Kawamura K, Jung J, Furutani H, Uematsu M. 2011. Latitudinal distributions of organic nitrogen and organic carbon in marine aerosols over the western North Pacific. *Atmospheric Chemistry and Physics* 11, 3037–3049. doi: [10.5194/acp-11-3037-2011](https://doi.org/10.5194/acp-11-3037-2011).
- Narukawa M, Kawamura K, Li SM, Bottenheim JW. 2008. Stable carbon isotopic ratios and ionic composition of the high-arctic aerosols: An increase in  $\delta^{13}\text{C}$  values from winter to spring. *Journal of Geophysical Research* 113(D2).
- Nel A. 2005. Air pollution-related illness: effects of particles. *Science* 308:804–806.
- Novakov T, Penner JE. 1993. Large contribution of organic aerosols to cloud-condensation-nuclei concentrations. *Nature* 365(6449):823–826.
- Paraskevopoulou D, Liakakou E, Gerasopoulos E, Theodosi C, Mihalopoulos N. 2014. Long-Term characterization of organic and elemental carbon in the PM<sub>2.5</sub> fraction: the case of Athens, Greece. *Atmospheric Chemistry and Physics* 14(23):13313–13325.
- Pavuluri CM, Kawamura K, Aggarwal SG, Swaminathan T. 2011a. Characteristics, seasonality and sources of carbonaceous and ionic components in the tropical aerosols from indian region. *Atmospheric Chemistry and Physics* 11(15):8215–8230.
- Pavuluri CM, Kawamura K, Swaminathan T, Tachibana E. 2011b. Stable carbon isotopic compositions of total carbon, dicarboxylic acids and glyoxylic acid in the tropical indian aerosols: Implications for sources and photochemical processing of organic aerosols. *Journal of Geophysical Research* 116(D18).
- Pavuluri CM, Kawamura K, Uchida M, Kondo M, Fu P. 2013. Enhanced modern carbon and biogenic organic tracers in northeast asian aerosols during spring/summer. *Journal of Geophysical Research: Atmospheres* 118(5):2362–2371.
- Ramanathan V, Crutzen PJ, Kiehl JT, Rosenfeld D. 2001. Atmosphere—aerosols, climate, and the hydrological cycle. *Science* 294(5549):2119–2124.
- Robinson AL, Donahue NM, Shrivastava MK, Weikamp EA, Sage AM, Grieshop AP, Lane TE, Pierce JR, Pandis SN. 2007. Rethinking organic aerosols: semivolatile emissions and photochemical aging. *Science* 315(5816):1259–1262.
- Rosenfeld D, Zhu Y, Wang M, Zheng Y, Goren T, Yu S. 2019. Aerosol-driven droplet concentrations dominate coverage and water of oceanic low-level clouds. *Science* 363(6427):eaav0566. doi: [10.1126/science.aav0566](https://doi.org/10.1126/science.aav0566).
- Rudolph J. 2002. Stable carbon isotope ratio measurements: A new tool to understand atmospheric processing of volatile organic compounds. *Nato Sci S Ss Iv Ear.* 16:37–42.
- Sciare J, Bardouki H, Moulin C, Mihalopoulos N. 2003. Aerosol sources and their contribution to the chemical composition of aerosols in the eastern mediterranean sea during summertime. *Atmospheric Chemistry and Physics* 3:291–302.
- Sciare J, Oikonomou K, Favez O, Liakakou E, Markaki Z, Cachier H, Mihalopoulos N. 2008. Long-term measurements of carbonaceous aerosols in the eastern mediterranean: Evidence of long-range transport of biomass burning. *Atmospheric Chemistry and Physics* 8(18):5551–5563.
- Simoneit BRT, Kobayashi M, Mochida M, Kawamura K, Lee M, Lim HJ, Turpin BJ, Komazaki Y. 2004. Composition and major sources of organic compounds of aerosol particulate matter sampled during the ace-asia campaign. *J Geophys Res-Atmos.* 109:D19S10. doi: [10.1029/2004JD004598](https://doi.org/10.1029/2004JD004598).
- Song J, Zhu M, Wei S, Peng Pa, Ren M. 2019. Abundance and  $^{14}\text{C}$ -based source assessment of carbonaceous materials in pm<sub>2.5</sub> aerosols in Guangzhou, South China. *Atmospheric Pollution Research* 10(1):313–320.
- Srivastava D, Vu TV, Tong S, Shi Z, Harrison RM. 2022. Formation of secondary organic aerosols from anthropogenic precursors in laboratory studies. *NPJ Climate and Atmospheric Science* 5:22. doi: [10.1038/s41612-022-00238-6](https://doi.org/10.1038/s41612-022-00238-6).
- Stock M, Cheng YF, Birmili W, Massling A, Wehner B, Müller T, Leinert S, Kalivitis N, Mihalopoulos N, Wiedensohler A. 2011. Hygroscopic properties of atmospheric aerosol particles over the Eastern Mediterranean: implications for regional direct



- radiative forcing under clean and polluted conditions. *Atmospheric Chemistry and Physics* 11(9):4251–4271.
- Stuiver M, Polach H. 1977. Discussion: reporting of  $^{14}\text{C}$  data. *Radiocarbon* 19(3):355–363.
- Szidat S, Jenk TM, Gäggeler HW, Synal HA, Fisseha R, Baltensperger U, Kalberer M, Samburova V, Reimann S, Kasper-Giebl A et al. 2004. Radiocarbon ( $^{14}\text{C}$ )-deduced biogenic and anthropogenic contributions to organic carbon (OC) of urban aerosols from zürich, switzerland. *Atmospheric Environment* 38(24):4035–4044.
- Theodosi C, Panagiotopoulos C, Nouara A, Zarmpas P, Nicolau P, Violaki K, Kanakidou M, Sempere R, Mihalopoulos N. 2018. Sugars in atmospheric aerosols over the Eastern Mediterranean. *Progress in Oceanography*, 163:70–81.
- Turekian VC. 2003. Concentrations, isotopic compositions, and sources of size-resolved, particulate organic carbon and oxalate in near-surface marine air at Bermuda during spring. *Journal of Geophysical Research* 108(D5), 4157. doi: [10.1029/2002JD002053](https://doi.org/10.1029/2002JD002053).
- Turekian VC, Macko S, Ballentine D, Swap RJ, Garstang M. 1998. Causes of bulk carbon and nitrogen isotopic fractionations in the products of vegetation burns: laboratory studies. *Chem Geol.* 152(1–2):181–192.
- Uchida M, Kumata H, Koike Y, Tsuzuki M, Uchida T, Fujiwara K, Shibata Y. 2010. Radiocarbon-based source apportionment of black carbon (BC) in pm<sub>10</sub> aerosols from residential area of suburban Tokyo. *Nuclear Instruments and Methods in Physics Research Section B: Beam Interactions with Materials and Atoms* 268(7–8):1120–1124.
- Uchida M, Mantoku K, Kobayashi T, Kawamura K, Shibata Y. 2023. Ultra small mass AMS  $^{14}\text{C}$  sample preparation and analyses at NIES-TERRA AMS facility. *Nuclear Instruments and Methods in Physics Research Section B: Beam Interactions with Materials and Atoms* 536:144–153.
- Uchida M, Shibata Y, Yoneda M, Kobayashi T, Morita M. 2004. Technical progress in ams microscale radiocarbon analysis. *Nuclear Instruments and Methods in Physics Research Section B: Beam Interactions with Materials and Atoms* 223–224:313–317.
- Urdiales-Flores D, Zittis G, Hadjinicolaou P, Osipov S, Klingmüller K, Mihalopoulos N, Kanakidou M, Economou T, Lelieveld J. 2023. Drivers of accelerated warming in mediterranean climate-type regions. *NPJ Climate and Atmospheric Science* 6:97. doi: [10.1038/s41612-023-00423-1](https://doi.org/10.1038/s41612-023-00423-1).
- Vrekoussis M, Liakakou E, Koçak M, Kubilay N, Oikonomou K, Sciare J, Mihalopoulos N. 2005. Seasonal variability of optical properties of aerosols in the Eastern Mediterranean. *Atmospheric Environment* 39(37):7083–7094.
- Wang Y, Pavuluri CM, Fu P, Li P, Dong Z, Xu Z, Ren H, Fan Y, Li L, Zhang Y-L. 2019. Characterization of secondary organic aerosol tracers over Tianjin, North China during summer to autumn. *ACS Earth and Space Chemistry* 3(10):2339–2352.
- Widory D, Roy S, Moullec YL, Goupil G, Cocherie A, Guerrot C. 2004. The origin of atmospheric particles in Paris: a view through carbon and lead isotopes. *Atmospheric Environment* 38: 953–961.
- Yttri KE, Simpson D, Bergström R, Kiss G, Szidat S, Ceburnis D, Eckhardt S, Hueglin C, Nøjgaard JK, Perrino C et al. 2019. The emep intensive measurement period campaign, 2008–2009: characterizing carbonaceous aerosol at nine rural sites in Europe. *Atmospheric Chemistry and Physics* 19(7):4211–4233.